



## RESEARCH ARTICLE

WILEY

# Analysis of leading edge protection application on wind turbine performance through energy and power decomposition approaches

Effi Latiffianti<sup>1,2</sup>  | Yu Ding<sup>1</sup>  | Shawn Sheng<sup>3</sup> | Lindy Williams<sup>3</sup> |  
Majid Morshedizadeh<sup>4</sup> | Marianne Rodgers<sup>4</sup>

<sup>1</sup>Department of Industrial and Systems Engineering, Texas A&M University, College Station, Texas, 77840, USA

<sup>2</sup>Department of Industrial and Systems Engineering, Institut Teknologi Sepuluh Nopember, Surabaya, East Java, Indonesia

<sup>3</sup>National Renewable Energy Laboratory, Golden, Colorado, 80401, USA

<sup>4</sup>Wind Energy Institute of Canada, Tignish, PEI C0B 2B0, Canada

## Correspondence

Yu Ding, Room 4016 ETB, Department of Industrial and Systems Engineering, Texas A&M University, College Station, Texas 77840, USA.

Email: [yuding@tamu.edu](mailto:yuding@tamu.edu)

## Funding information

Department of Energy, Grant/Award Number: DE-AC36-08GO28308; DIKTI-Funded Fulbright Scholarship; NSF, Grant/Award Numbers: IIS-1741173 I, CCF-1934904

## Abstract

Wind power production is driven by, and varies with, the stochastic yet uncontrollable wind and environmental inputs. To compare a wind turbine's performance, a direct comparison on power outputs is always confounded by the stochastic effect of weather inputs. It is therefore crucial to control for the weather and environmental influence. Toward that objective, our study proposes an energy decomposition approach. We start with comparing the change in the total energy production and refer to the change in total energy as delta energy. On this delta energy, we apply our decomposition method, which is to separate the portion of energy change due to weather effects from that due to the turbine itself. We derive a set of mathematical relationships allowing us to perform this decomposition and examine the credibility and robustness of the proposed decomposition approach through extensive cross-validation and case studies. We then apply the decomposition approach to Supervisory Control and Data Acquisition data associated with several wind turbines to which leading-edge protection was carried out. Our study shows that the leading-edge protection applied on blades may cause a small decline to the power production efficiency in the short term, although we expect the leading-edge protection to benefit the blade's reliability in the long term.

## KEYWORDS

data science, effects decomposition, leading-edge protection, statistical and machine learning, turbine performance analysis

## 1 | INTRODUCTION

In the past decade, wind power has been a rapidly growing source of renewable energy worldwide. In 2020, wind energy accounted for about 8.4% of the total U.S. utility-scale electricity generation.<sup>1</sup> The cost of wind energy generation depends on both the reliability and the performance of wind turbines. Advancements in wind turbine technology have been continuously introduced in attempts to improve efficiency and reduce cost. Despite the advancements, wind turbine performance inevitably declines with age. Typically, the portion of the performance loss could be attributed to gradual deterioration, such as fouling of the blades and a gradual reduction in component efficiencies.<sup>2</sup> It is therefore essential to

This is an open access article under the terms of the [Creative Commons Attribution](https://creativecommons.org/licenses/by/4.0/) License, which permits use, distribution and reproduction in any medium, provided the original work is properly cited.

© 2022 The Authors. *Wind Energy* published by John Wiley & Sons Ltd.

understand how turbine performance changes over time as well as how turbine technologies compare to each other. Performance analysis helps wind farm operators to monitor turbine performance as they age and is especially useful to discern the impact of certain technical changes undertaken. Understanding the impact of technical changes helps identify root causes behind performance deterioration or the best practice for maintaining a wind turbine's production efficiency.

Exposure to harsh environmental conditions and high wind speed can cause damage to the leading-edges of wind turbine blades, which in turn compromises the blades' performance. In response to this phenomenon, the Wind Energy Institute of Canada (WEICan) examined the adhesion, resistance to erosion, and durability of several leading-edge protection (LEP) products in a field test on the blades of wind turbines, housed in their Wind R&D Park at North Cape on Prince Edward Island, Canada. The study commenced in summer 2016 with four different types of LEP applied on five turbines. A drone inspection after 3 years of operation revealed signs of damage and resulted in repairs being done on four of the turbines.

Based on the reviews of existing protection solutions,<sup>3</sup> there appears to be several common failure themes, including poor adhesion, poor manufacturing, and application techniques that introduce defects and hence initiation points for erosion. These can be possible explanations for the defects found through the drone inspection. There does not appear to be strong evidence pointing to significant manufacturing defects of the LEP tapes. However, the application of the LEP tapes to the blades likely introduces imperfections, such as wrinkles and air pockets, which can reduce the adhesion of the bond. After the application and repair of the LEP, a question emerged about how much these actions truly affected the performance of the wind turbines. To shed some light on this question, a joint research team was formed, comprising researchers from Texas A&M University (TAMU), National Renewable Energy Laboratory (NREL), and WEICan, and to conduct a wind turbine performance analysis.

Comparing power outputs is a common approach to evaluating wind turbine performance.<sup>4–9</sup> Wind practitioners are aware that when using power comparison directly, the influence of the stochastic weather effects confounds the final finding, making it harder to quantify the change in terms of a turbine's intrinsic performance. Several approaches have been proposed in response to the need to filter out the weather effects. One approach is to control the effects from environmental factors by applying a kernel plus method that allows incorporation of multivariate environmental factors in a power model.<sup>5</sup> Another approach is to use a covariate matching<sup>6</sup> to filter the data so that the pair of data under comparison are statistically comparable. Furthermore, Ding et al<sup>7</sup> devised a three-step wind turbine performance quantification procedure, which adopts both of the earlier techniques<sup>5,6</sup> in its first and second steps and adds a function curve comparison in its third step. The last step also serves the purpose of uncertainty quantification, which associates a confidence interval with the performance comparison. In this article, we use the turbine performance quantification method proposed in Ding et al<sup>7</sup> as one of the primary approaches.

To provide a better interpretation and also cross-validate the robustness of the results, our research team further developed an energy decomposition method. This energy decomposition method allows the change in total energy production to be separated into two terms—one that represents what is caused by the change in the weather conditions and another that represents what is caused by the wind turbine itself (i.e., a turbine's intrinsic performance change). In the end, the two methods, the one in Ding et al<sup>7</sup> and the new energy decomposition method, produce rather consistent results, which provides verification for the conclusions reached in this article. Using these tools, the team investigates how the blade-related technical action affects wind turbines performance.

The rest of the article is organized as follows. In Section 2, we explain the application background and the data sets used in this study. In Section 3, we provide the details about the energy decomposition method and outline the overall procedure used in the study. In Section 4, we present and discuss the results of the case study and also analyze the various aspects concerning the methods proposed in Section 3. Finally, we summarize this work in Section 5.

## 2 | BACKGROUND AND DATA

Figure 1 presents the layout of the five wind turbines in the wind farm. This small wind farm operates in a coastal environment and extreme temperatures. The total capacity of the wind farm is 10 MW with each turbine belonging to the same model in the 2 MW class. The cut-in, rated, and cut-out wind speeds are 4 m/s, 10 m/s, and 25 m/s, respectively. Although there is a meteorological mast on this wind farm, all data used in the analysis were recorded from individual turbine measurements.

The data sets were collected from January 2013 through October 2020; 10-min averages, minimum and maximum values, and standard deviations were recorded. The original data are available for seven years. Because the first blade-related technical action took place in the summer of 2016, we backdated to 1 year prior to the first technical action for our data use. In other words, we use the data from June 2015 and onward, which is over 5 years. The data recordings are of high quality in general, as there are only small amounts of missing data.

For each point in the data set, we have a pair of an output variable denoted by  $y$  and a vector of input variables denoted by  $x$ . The output variable is the instant active power of the turbine. The input variables include the following environmental measurements: wind speed ( $V$ ), ambient temperature ( $T$ ), and wind direction ( $D$ ). Using the wind direction data, the standard deviation of wind direction ( $sdD$ ) is computed, whereas using the wind speed data, the turbulence intensity ( $TI$ ) is computed through the following formula:

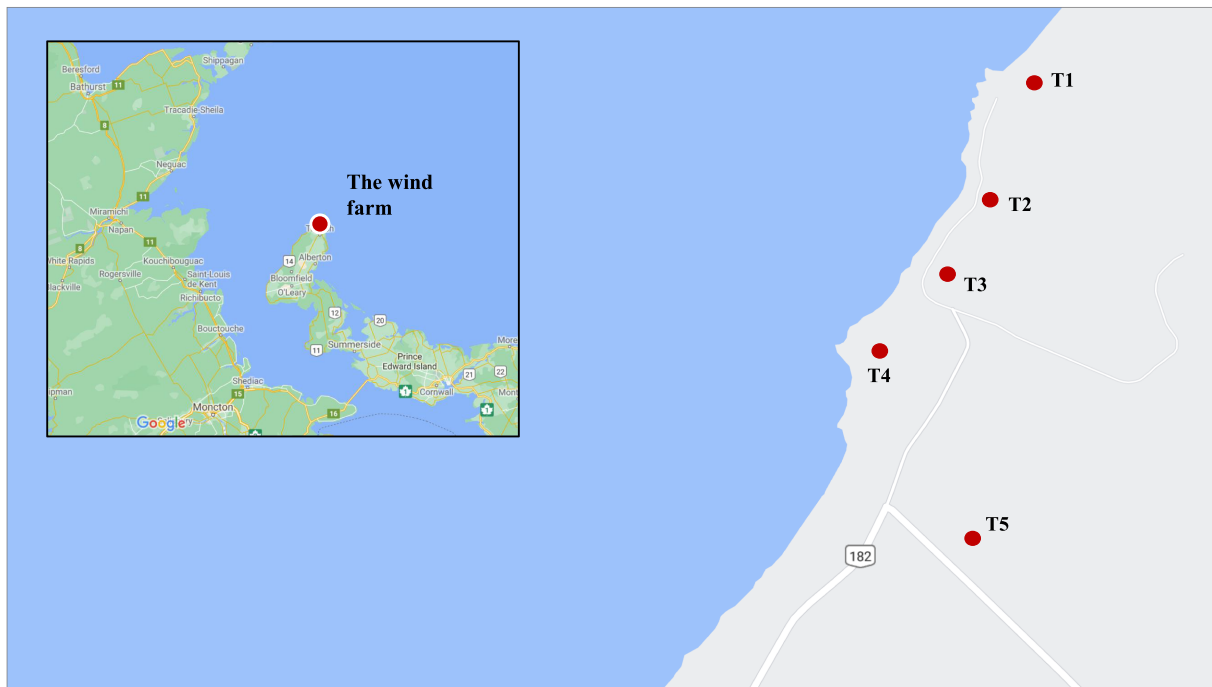


**FIGURE 1** Wind turbine layout in the wind farm and the location of the wind farm, based on the Google map<sup>10</sup>

**TABLE 1** The timeline of the technical changes

Time	June–Aug. 2016	Oct.–Nov. 2017	Aug.–Sept. 2019
Technical action	#1: LEP application	#2: Blade repainting	#3: LEP repair
Affected turbines	All	T1	T1, T3, T4, T5

**TABLE 2** The common periods of wind turbine performance analysis

June 2015–May 2016	Sept. 2016–Sept. 2017	Dec. 2017–Aug. 2019	Sept. 2019–Aug. 2020
Period 1	Period 2	Period 3	Period 4
No upgrade	Evaluate LEP application	Evaluate LEP + repainting	Evaluate Repainting + LEP repair

$$Tl_i = \frac{sdV_i}{V_i} \text{ for } i = 1, \dots, n, \quad (1)$$

where  $V_i$  is the average wind speed and  $sdV_i$  is the wind speed standard deviation at time stamp  $i$ . Altogether, five external variables are used. Two more variables, the rotor speed ( $G$ ) and blade pitch angle ( $PA$ ), are also explored, but they are not used in the power model for performance analysis because their measurements are considered internal to the turbines.

There were three blade-related actions during the 5-year period, which are the application of LEP tapes and paints, blade repainting, and the LEP repair. The first technical action was performed on all turbines, but the second and third technical actions were not performed on some of the turbines. The blade action information is presented in Table 1.

The three actions in Table 1 separate the 5-year study period into four segments (see Table 2). In both tables, the time for each blade action is given in 3-, 2-, or 1-month windows. This is because the actions on the five turbines took place at different times. Altogether it took 1–3 months to complete an action for all intended turbines.

One may define the periods under comparison differently for different analyses. When comparing one wind turbine to another, we use a common time window for both turbines, and this common window is wider in order to accommodate the action time windows of both turbines. When comparing the period before and after a technical action for a wind turbine itself, we can use the periods immediately before and after the action of a single turbine. Consequently, the action window is narrower.

Please note that for parts of the analysis, especially those involving pairwise wind turbine performance comparison, we use four of the turbines (T1–T4) while excluding T5. T5 is located more inland and its wind inflow conditions are noticeably different from those of the other four. Additionally, T5 was not operating during a sizeable portion of Period 4 and was derated even more significantly for the rest of the period.

### 3 | METHODOLOGY

Mathematically, the performance evaluation problem is to compare a pair of data sets  $D^{(1)} = \{\mathbf{X}^{(1)}, \mathbf{y}^{(1)}\}$  and  $D^{(2)} = \{\mathbf{X}^{(2)}, \mathbf{y}^{(2)}\}$ , where  $\mathbf{X}^{(k)} = \{\mathbf{x}_1^{(k)}, \dots, \mathbf{x}_{n_k}^{(k)}\}$  represents the matrix of inputs,  $\mathbf{y}^{(k)} = \{y_1^{(k)}, \dots, y_{n_k}^{(k)}\}$  is the vector of power output,  $n_k$  is the number of the data pairs in data set  $k$ , and  $k = 1, 2$ . It is easier to envision the use of these notations when the two data sets are from one turbine over two different time periods (for instance, before and after a technical action). But the same notations can also be used for comparing two different turbines. Hereinafter, we say that  $D^{(1)}$  is for Period 1 and  $D^{(2)}$  is for Period 2, where Period 1 and Period 2 are the general reference to the periods before and after a technical action, not to be confused with the specific periods defined in Section 2. Please see an illustration in Figure 2.

We assume that our Supervisory Control and Data Acquisition (SCADA) data sets come from the underlying models, given by

$$y_i^{(k)} = f^{(k)}(\mathbf{x}_i^{(k)}) + \epsilon_i^{(k)}, \quad k = 1, 2 \quad i = 1, \dots, n_k, \quad (2)$$

where  $f^{(k)}(\cdot)$  is a power function associated with each period, which needs to be estimated from the respective data set, and  $\epsilon_i^{(k)} \sim \mathcal{N}(0, \sigma_\epsilon^2)$ , with  $\sigma_\epsilon^2$  as the variance of the noise.

This section explains two methods used in the subsequent analysis. The first one is based on an existing method,<sup>7</sup> which compares the power output while controlling for the weather effects. This existing method is already implemented in an  $\mathbb{R}$  package and can be called upon readily, but we explain the basic idea and algorithmic components of this method in Section 3.1. The second approach is to compare the change in energy production, rather than the change in power. The difference in energy production is referred to as delta energy and denoted by  $\Delta E$ . It is on this delta energy that we develop a decomposition method to separate the portion due to weather from the portion due to the wind turbine itself. The difference quantified in the power-based approach in Ding et al<sup>7</sup> has already had the weather effect controlled for and is thus the difference due to the turbine itself. It is on this turbine portion that we expect the two methods to give consistent and comparable outcomes.

The procedure proposed by Ding et al<sup>7</sup> will be referred to as delta power quantification or Approach #1, while the quantification of energy difference using the proposed decomposition method will be referred to as delta energy quantification or Approach #2.

#### 3.1 | Delta power quantification

Because Approach #1 is a published work, our purpose here is to provide a high-level recap to make this article self-sustained. We try to be as brief as possible.

Approach #1 consists of three steps as presented in Figure 3. Intuitively, the first step addresses the question of which input variables to use, the second step addresses the question of which data to use, and the third step addresses the question of how to conduct comparisons and quantify uncertainty.

Step 1 is known as variable subset selection, or simply subset selection. It screens the available signals from SCADA data through a forward stepwise selection and selects the significant subset of input variables to be used in the resulting power function model. The variables are chosen to produce the smallest root-mean-squared error (RMSE) or the mean absolute error (MAE) based on a tenfold cross-validation. While the SCADA data contain a large number of signals, Step 1 produces a small number of input variables for power modeling, which are  $V$ ,  $T$ ,  $sdD$ ,  $D$ , and  $TI$ .

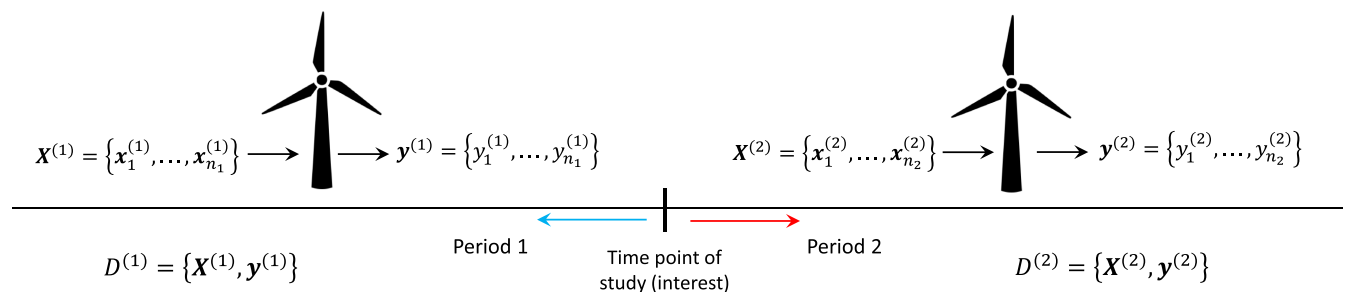
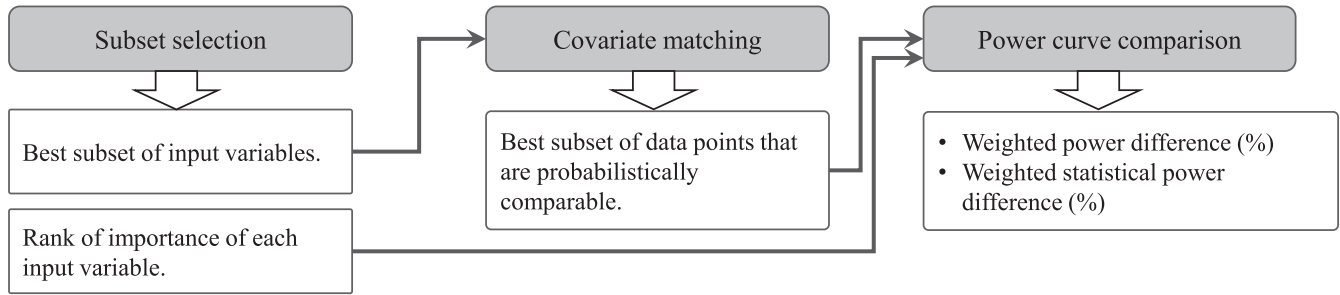


FIGURE 2 Notations and terminology illustrated

**Step 1: Which input variables to be used in the model?**

**Step 2: Which data points are used to train the model?**

**Step 3: How to compare functional curves and quantify uncertainty?**



**FIGURE 3** Three steps of power difference quantification using Approach #1

Step 2 is known as covariate matching<sup>6</sup> and aims at picking data points for making the weather conditions probabilistically comparable after a technical action. The technique used in the step falls under the broad statistical methodological framework known as *causal inference*,<sup>11</sup> which originated from social science studies where a *natural experiment* with observational data, instead of a *controlled experiment*, needs to be handled.<sup>4</sup>

Step 3 is to use a Gaussian process-based (GP) power function model and estimate the parameters of the GP model based on the variable subset selected in Step 1 and data subset selected in Step 2. The GP-based method is a generic data science method<sup>12</sup> capable of comparing two nonparametric functional curves through a statistical hypothesis test. For turbine performance comparison, the two nonparametric functional curves are the respective power functions associated with the wind turbines (i.e., the  $f$ 's in Equation (2)). Because the GP-based method enables a statistical hypothesis test on functional curves, it naturally presents a confidence interval on the comparison results and thus quantifies the uncertainty of the comparison.

All three steps can be performed by calling the `ComparePCurve` function in the `DSWE` package in R.<sup>13</sup> The `ComparePCurve` function returns multiple versions of power difference, including the weighted difference and the weighted *statistical* difference. The weighted power difference is obtained by

$$\Delta \hat{Y}_{\text{weighted}} = \frac{\sum_{i=1}^{n_{\text{test}}} P_i \times (\hat{f}^{(2)}(\mathbf{x}_i) - \hat{f}^{(1)}(\mathbf{x}_i))}{\sum_{i=1}^{n_{\text{test}}} P_i \times \hat{f}^{(1)}(\mathbf{x}_i)}, \quad (3)$$

where  $n_{\text{test}}$  is the number of data points being compared,  $P_i$  is the relative frequency associated with a specific input condition  $\mathbf{x}_i$ , and  $\hat{f}$  (with the hat notation) is the *estimated* power function. The above difference is called “weighted” difference because it is the power difference weighted by the relative frequency of the weather conditions.

The weighted *statistical* difference is likewise defined but the main difference is that the weighted statistical difference accumulates only the portions that are beyond the  $100(1 - \alpha)\%$  confidence band, when it comes to counting the power difference. The use of statistical significant difference is to make the comparison robust by weeding out the portions that may have been caused by random fluctuation in the data.<sup>7</sup> The original “weighted difference” is considered as an *absolute* difference.

Figure 4 illustrates the distinction of the two power differences. The blue solid line is the power difference function plotted against wind speed, namely  $\hat{f}^{(2)}(\mathbf{x}_i) - \hat{f}^{(1)}(\mathbf{x}_i)$ . The right panel shows the absolute difference – that counts every aspect of the differences, which is the summation of all orange regions. The left panel shows the statistical difference at the 95% significance level, which only counts the portions beyond the 95% confidence band; that is the blue region. Apparently, the statistical difference tends to be smaller than the absolute difference. The distinction between these differences is considered the effect of random fluctuation in data.

As mentioned earlier, these power differences resulting from Approach #1 have already excluded the weather effects through its analysis procedure and hence represent the performance change associated with the wind turbines. In this study, we use the weighted difference when cross-validating the results with those from the energy decomposition method (next subsections), and use the weighted statistical difference to understand how much the difference is beyond the natural fluctuation.

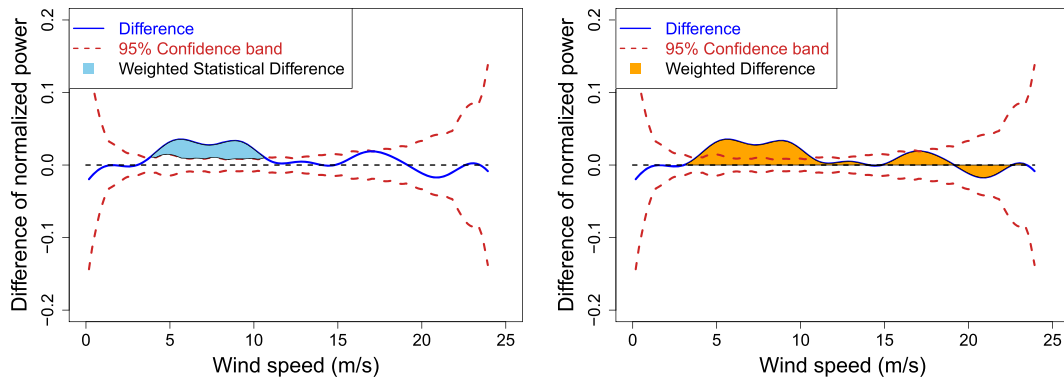


**FIGURE 4** Two versions of power difference—weighted statistical difference (left panel, blue region) and weighted absolute difference (right panel, summation of the orange regions)

### 3.2 | Delta energy quantification

Practitioners tend to use energy differences to quantify a wind turbine's performance change. One example is the use of annual energy performance (AEP) to quantify production losses when turbine performance declines.<sup>14</sup> The use of delta energy can be readily derived for our turbine performance purpose using the notations defined in Equation (2).

The so-called direct energy comparison, the simplest and most straightforward approach, is to calculate the delta energy (the difference between total energy recorded in the two data sets) such as

$$\Delta E_{obs} = \sum_{i=1}^{n_2} y_i^{(2)} t_i - \sum_{i=1}^{n_1} y_i^{(1)} t_i, \quad (4)$$

where  $t_i$  is the duration starting at time  $i$  and  $y_i$  is the average power for that duration. We label this delta energy term as  $\Delta E_{obs}$ , the subscript of which emphasizes that it is the *observed* energy difference between two data sets.

Using the power function,  $\hat{f}^{(k)}$ , in Equation (2), we can estimate  $\Delta E_{obs}$  as

$$\Delta \hat{E} = \sum_{i=1}^{n_2} \hat{f}^{(2)}(\mathbf{x}_i^{(2)}) t_i - \sum_{i=1}^{n_1} \hat{f}^{(1)}(\mathbf{x}_i^{(1)}) t_i. \quad (5)$$

We refer to  $\Delta \hat{E}$  as the *smoothed* version of  $\Delta E_{obs}$  because once using the power function,  $\hat{f}^{(k)}(\cdot)$ , the noise effect of  $\epsilon$  is smoothed out from the raw data. Understandably,  $\Delta E_{obs}$  and  $\Delta \hat{E}$  are close to each other, as they only differ in the amount of  $\epsilon$ .

The delta energy, both observed and smoothed, represents the total energy change associated with the two data sets (for two time periods or two wind turbines). It contains not only a turbine's performance change but also the energy change due to weather effects. To make the delta energy approach useful for turbine performance analysis, it is critical to decompose the total delta energy into its weather portion and turbine portion, namely

$$\Delta E = \Delta E_{weather} + \Delta E_{turbine}, \quad (6)$$

where  $\Delta E_{weather}$  represents the weather effect and  $\Delta E_{turbine}$  represents the energy change due to a turbine's own effect. The challenge here is that only the left-hand side,  $\Delta E$ , is observable in the data, whereas the terms in the right-hand side,  $\Delta E_{weather}$  and  $\Delta E_{turbine}$ , are not directly observable from the data, but will have to be estimated. Naturally, we can make use of the smoothed version of the delta energy,  $\Delta \hat{E}$ . The decomposition in Equation (6) implies the following:

$$\Delta \hat{E} = \Delta \hat{E}_{weather} + \Delta \hat{E}_{turbine}. \quad (7)$$

The question is how to compute the estimates of the two delta energy terms for weather and for the wind turbine, namely,  $\Delta \hat{E}_{weather}$  and  $\Delta \hat{E}_{turbine}$ , respectively.

Imagine that we have an ideal wind turbine for which the performance does not change over time. Let  $\hat{f}(\cdot)$  be the power function representing the performance of that turbine. It is not difficult to see that the weather effect can be estimated by computing the delta energy produced by this ideal turbine over two sets of weather conditions,  $\mathbf{x}^{(1)}$  and  $\mathbf{x}^{(2)}$ :

$$\Delta \hat{E}_{weather} = \sum_{i=1}^n \left( \hat{f}(\mathbf{x}_i^{(2)}) - \hat{f}(\mathbf{x}_i^{(1)}) \right) t_i. \quad (8)$$

In reality, we do not have this ideal turbine represented by a single, unified power function model,  $\hat{f}(\cdot)$ , but two power functions associated with Period 1 and Period 2:  $\hat{f}^{(1)}(\cdot)$  and  $\hat{f}^{(2)}(\cdot)$ , respectively. This raises the question of which power function should be used in Equation (8).

We believe a reasonable way to estimate is to use both power functions and then take an average. This is to say, we first compute the energy production difference resulting from the turbine, represented by  $\hat{f}^{(1)}(\cdot)$ , when it is experiencing two weather conditions. Then, we compute the energy production resulting from the other turbine, represented by  $\hat{f}^{(2)}(\cdot)$ , when it is experiencing the same two weather conditions. The average of the energy production differences is treated as the estimate of  $\Delta \hat{E}_{weather}$ . Mathematically, this estimate is expressed as

$$\Delta \hat{E}_{weather} = \frac{1}{2} \left( \sum_{i=1}^{n_2} \hat{f}^{(1)}(\mathbf{x}_i^{(2)}) t_i - \sum_{i=1}^{n_1} \hat{f}^{(1)}(\mathbf{x}_i^{(1)}) t_i \right) + \frac{1}{2} \left( \sum_{i=1}^{n_2} \hat{f}^{(2)}(\mathbf{x}_i^{(2)}) t_i - \sum_{i=1}^{n_1} \hat{f}^{(2)}(\mathbf{x}_i^{(1)}) t_i \right). \quad (9)$$

Now let us turn to the turbine effect. Again, imagine that we can subject two turbines to exactly the same weather conditions, denoted by  $\mathbf{x}_i$ . The two turbines are represented by two different power functions,  $\hat{f}^{(1)}$  and  $\hat{f}^{(2)}$ , respectively. Then, the turbine effect can be estimated by computing the delta energy produced by the two turbines under the same weather conditions:

$$\Delta \hat{E}_{turbine} = \sum_{i=1}^n \left( \hat{f}^{(2)}(\mathbf{x}_i) - \hat{f}^{(1)}(\mathbf{x}_i) \right) t_i. \quad (10)$$

Once again, the actual weather conditions are not exactly the same. Rather, there are two sets of weather conditions,  $\mathbf{x}^{(1)}$  and  $\mathbf{x}^{(2)}$ . Instead of using either one of them (a hard choice to make), the treatment here is again to use both and then take an average. As such, our  $\Delta \hat{E}_{turbine}$  is

$$\Delta \hat{E}_{turbine} = \frac{1}{2} \left( \sum_{i=1}^{n_1} \hat{f}^{(2)}(\mathbf{x}_i^{(1)}) t_i - \sum_{i=1}^{n_1} \hat{f}^{(1)}(\mathbf{x}_i^{(1)}) t_i \right) + \frac{1}{2} \left( \sum_{i=1}^{n_2} \hat{f}^{(2)}(\mathbf{x}_i^{(2)}) t_i - \sum_{i=1}^{n_2} \hat{f}^{(1)}(\mathbf{x}_i^{(2)}) t_i \right). \quad (11)$$

It is easy to verify that the decomposition relationship in Equation (7) holds strictly when using  $\Delta \hat{E}_{weather}$  in Equation (9) and  $\Delta \hat{E}_{turbine}$  in Equation (11). This can be done by simply adding the right-hand sides of Equation (9) and Equation (11), which gives the right-hand side of Equation (5).

To provide  $\Delta \hat{E}_{weather}$  and  $\Delta \hat{E}_{turbine}$  in percentage, we compare their values with the averaged total energy observed in both data sets, meaning the averaged total energy used as the baseline in the denominator. The delta energy percentage expressions are

$$\% \Delta \hat{E}_{weather} = \frac{\Delta \hat{E}_{weather}}{\frac{1}{2} \left( \sum_{i=1}^{n_2} y_i^{(2)} t_i + \sum_{i=1}^{n_1} y_i^{(1)} t_i \right)} \times 100\%, \quad (12)$$

$$\% \Delta \hat{E}_{turbine} = \frac{\Delta \hat{E}_{turbine}}{\frac{1}{2} \left( \sum_{i=1}^{n_2} y_i^{(2)} t_i + \sum_{i=1}^{n_1} y_i^{(1)} t_i \right)} \times 100\%. \quad (13)$$

### 3.3 | Implementation details for the delta energy approach

There are a few implementation details to be sought out for the delta energy approach and the subsequent decomposition. The first is what type of power functions to use. There has been a wide range of machine-learning methods used, including support vector regression,<sup>15,16</sup> k-nearest neighbor (kNN),<sup>17</sup> Gaussian Process-based models,<sup>12,18–20</sup> monotonic regression,<sup>21</sup> and artificial neural network (ANN)<sup>22</sup>; please see Chapter 5 of Ding<sup>4</sup> for a comprehensive discussion on this topic. Our implementation uses a power function model based on a tempGP model, which, through intensive testing, shows the best performance among a large family of machine-learning-based power models.<sup>18</sup> This tempGP-based power function model takes the same five input variables as found in Step 1 of Approach #1 (i.e.,  $V$ ,  $T$ ,  $sdD$ ,  $D$ , and  $TI$ ).

The second implementation detail is data preprocessing for data synchronization and imputation. Data synchronization ensures both data sets have comparable sizes. Synchronization is important because energy is time-dependent. The more data points one has for a period, the higher the total energy expected for that period. Comparing two data sets of different sizes makes the comparison unfair. In our instance, when two data sets come from two different wind turbines at the same period of time, we synchronize the time stamp so that both subsets consist of only points at the same time stamps, and hence they have the same number of data points. When the pair of data are from one turbine at different time periods, we remove data points from the data set of the larger size until both have the same number of data points. The choice of which data points to remove may vary. In our study, we started with the data points where the wind speed is zero or otherwise the lowest. This way, it affects the energy output the least.

After the synchronization, each data set may contain a subset of data points where the turbine is not in operation, under which the power output will be zero or negative despite a valid wind speed between the cut-in and cut-out speeds. On these subsets of invalid power outputs, we perform imputation using the following rule.

$$y_i^{(k)} = \begin{cases} 0, & \text{if } 0 \leq V_i < V_{ci} \text{ or } V_i > V_{co} \\ \hat{f}^{(k)}(x_i), & \text{if } V_{ci} \leq V_i \leq V_r \\ \text{rated power,} & \text{if } V_{co} \geq V_i > V_r, \end{cases} \quad (14)$$

where  $V_i$  is the wind speed at time  $i$  and  $V_{ci}$ ,  $V_{co}$ , and  $V_r$  are the cut-in, cut-out, and rated wind speeds, respectively. At the end of the imputation, both data sets are of the same size with valid power output values at all points.

## 4 | RESULTS AND DISCUSSION

### 4.1 | Impact of LEP application

The first step of our analysis was to use Approach #1 (the delta power approach) to analyze the whole data set. In fact, we added one extra year's worth of data right before Period 1 and labeled the extra data as Period 0. The purpose of adding Period 0 data is to let us observe how each wind turbine changes when no blade technical action was undertaken.

Using Approach #1 is straightforward. As explained in Section 3.1, this can be done by calling the `ComparePCurve` function in the `DSWE` package in R.<sup>13</sup> The `ComparePCurve` function takes in the data in two periods and outputs the weighted power difference and the weighted statistical power difference. The results are presented in Table 3.

Because we have five periods and five wind turbines, the comparison we conducted here is a period-based comparison for each individual turbine. To reduce the number of the comparisons, we treat Period 2, the period right after the LEP application, as the base period. In other words, the performance of a turbine in that period is set to zero. Then, all other periods of the same turbine are compared with the turbine's own Period 2 performance. This way, we conducted four comparisons per turbine. By contrast, a complete enumeration of all pairwise comparisons for a single turbine would be 10 comparisons, but the results would have been the same.

In the comparison, a positive value means that the said period has a better performance than Period 2 for the said turbine. Take T1 as an example. Its performance in Period 1 (the weighted difference) is 2.06%. This means that T1 performed 2.06% better in Period 1 than in Period 2 in terms of its production efficiency, defined as unit-time energy production under the same weather condition. Alternatively, one can say that T1's performance decreased 2.06% when going from Period 1 to Period 2.

When the two comparison periods do not include Period 2, say, as one compares Period 1 and Period 4, one can simply take the difference between the performance values listed respectively for the two periods. As both values use Period 2 as the common baseline, the difference between them would be the same as if we had used the two periods in a direct pairwise comparison (we in fact did this and confirmed that they

**TABLE 3** Power difference over all periods for all five turbines

Turbine	Weighted power difference				Weighted statistical power difference			
	Period 0	Period 1	Period 3	Period 4	Period 0	Period 1	Period 3	Period 4
T1	1.22%	2.06%	1.86%	2.17%	1.20%	1.07%	0.89%	1.49%
T2	1.80%	0.89%	1.88%	7.10%	1.74%	0.29%	0.62%	5.76%
T3	2.38%	1.91%	1.72%	3.90%	2.20%	0.84%	0.93%	2.45%
T4	-1.76%	-2.52%	-3.31%	0.82%	-1.23%	-1.96%	-1.82%	0.31%
T5	-0.50%	1.53%	1.55%	0.83%	-0.04%	1.08%	0.95%	0.43%



are indeed numerically consistent). Still, consider T1 as the example. Its Period 1 lists 2.06% and Period 4 lists 2.17%, so the difference between these two periods is 0.11% (Period 4 is better).

The right-hand side of Table 3 presents the values of weighted statistical difference, which remove from the performance quantification the variability caused by random fluctuation in the data. It is not surprising to see that the weighted statistical differences all become smaller in magnitude (in absolute values). The difference between the left-hand-side values and their right-hand-side counterparts can be as large as 1.49% in Table 3.

We believe that the weighted statistical differences provide a more robust metric for decision-making. To visualize the performance changes of each wind turbine along the time axis, we plot the weighted statistical differences in Figure 5 and connect them with lines. It is easy to spot that Period 2 is used as the common baseline for all turbines, as all performances are reset to zero for that period.

Based on the results, the LEP application did not always bring a positive change to a wind turbine's immediate production efficiency. In fact, four of the five turbines saw a small decrease in performance, in the range of [0.29%, 1.08%] and with an average of 0.82%. This decrease is not entirely unexpected. Earlier research<sup>23</sup> indicated that applying LEP could possibly alter the profile of the blade, increase drags, and then lead to some small decrease in turbine performance. In that study,<sup>23</sup> the performance decrease was reported to be 0.5%, not much different from what we observed here. On the other hand, this decrease does not necessarily mean that LEP applications had no benefit, as the LEP benefit is likely in the longer term, protecting the blades from further damage or even catastrophic failures. In T2 and T3, one can observe a slowdown in the performance decline after LEP application if comparing the respective P0–P1 performance change with the P1–P2 change.

Among the five turbines, T4 is the only one with a positive performance change after LEP application. There were four types of LEP applied to the five turbines, named A, B, C, and D. Type A was applied to T1 and T5, whereas types B, C, and D were applied to T2, T3, and T4, respectively. It is possible that the LEP materials are the reason why T4 is different. Type D LEP may warrant a closer look for researchers to decide whether applying it is indeed advantageous than other LEP types.

In terms of the second technical action, the power differences indicate some improvement in all four turbines except T4. Unlike the first technical action, the repainting was not the only action performed on the turbines during the time. There were other problems that required maintenance actions. Also note that when the second action was undertaken, it was only applied to T1. Considering all non-ideal conditions making comparison and quantification difficult, we decide not to do a detailed analysis of the repainting.

In contrast to the first technical action of LEP application, four of the wind turbines showed positive performance change after the LEP repair while only T5 deteriorated. What surprised us is that while the LEP repair was not undertaken on T2, its performance change was also positive and most pronounced. Inspection showed that T2 had the least eroded blades among all of the wind turbines. Nonetheless, such inspection result of T2 only suggested either a smaller decline or no detectable decline, rather than a positive improvement. It is apparent that the improvement in T2 was due to something else. We are also cognizant of the possibility of model bias in performance quantification. These considerations motivate us to carry out further investigations focusing on T2 and centering at the LEP repair time point. This further investigation includes validation and sensitivity analysis as well as decomposing the total energy change into turbine and weather effects. We also look into T2's gearbox and drivetrain data to understand the reason behind T2's improvement.

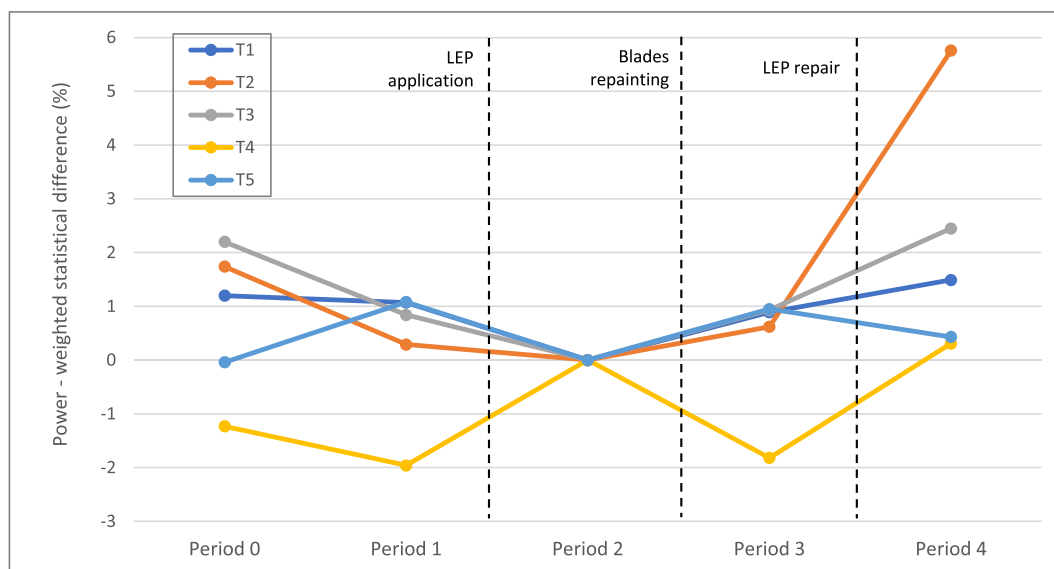


**FIGURE 5** Weighted statistical power difference representing turbine performance change across different periods

## 4.2 | Validation and sensitivity analysis

The objective of this analysis is to validate the results we previously obtained from Approach #1 and to understand how sensitive the results are to the length of the comparison periods (before and after an action). For the validation, we compare the weighted power difference from Approach #1 and that from the International Electrotechnical Commission (IEC) binning method.<sup>24</sup> We choose the binning method simply because it is considered the default option in the wind industry.<sup>25</sup> For the sensitivity analysis, we compare the weighted power difference for data periods of various lengths, specifically from 1 to 12 months.

In obtaining the power differences using the binning method, we directly calculate the weighted power difference using all data points in the two data sets involved. The power function is the power curve broadly used in the wind industry and established using the corrected wind speed ( $V'$ ) and the power output ( $y$ ). The corrected wind speed ( $V'$ ) is obtained by incorporating temperature correction to the measured wind speed ( $V$ ), a practice similar to air density correction.

The first validation test is to compare the binning-based analysis outcomes with those from Approach #1 reported earlier. The data sets used are 12 months before and after a technical action. As mentioned earlier, the focus on technical action here is the LEP repair, meaning that the power difference is obtained by comparing Period 3 and Period 4 for each wind turbine, with Period 3 treated as the baseline. The results are presented in Table 4. For all five turbines, the weighted power differences from both methods seem to cross-validate each other. The small gaps between the results of the two methods are reasonable due to the differences in procedures and the power function models used.

The sensitivity analysis is performed for each of the five turbines by shortening the periods before and after the technical action by 1 month at a time, until the time duration reaches 1 month on either side of the technical action. There are altogether 12 tests, corresponding to the 12 comparison period lengths, each of which are analyzed by using both Approach #1 and the binning method. As the results from the five turbines are consistent, we choose to present only the result associated with T2 in Figure 6 while omitting the same plots for other turbines to save space.

While implementing Approach #1, we found that when the period is not adequately long, there will not be enough data points left at the end of the covariate matching (Step 2). Consequently, the functional curve comparison in Step 3 can only be performed to the small subset left. This

**TABLE 4** The weighted power difference from Approach #1 and the binning method

	Weighted power difference				
	T1	T2	T3	T4	T5
Approach #1	1.19%	5.02%	-0.89%	3.18%	-2.57%
IEC binning	1.39%	4.93%	-0.87%	3.08%	-3.07%

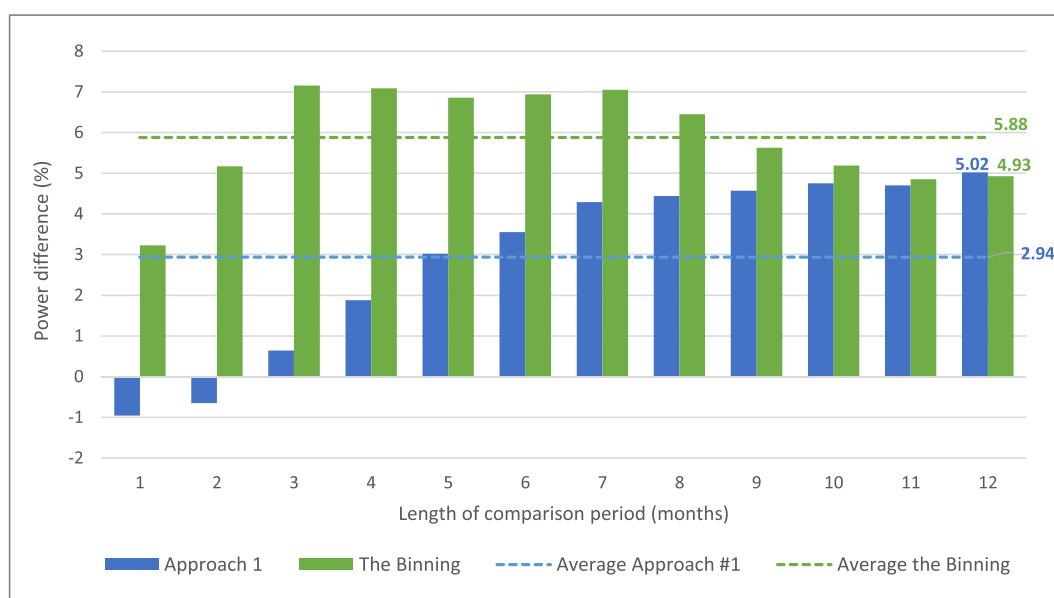


**FIGURE 6** Sensitivity analysis under different lengths of the comparison periods. The comparison was performed between Period 3 and Period 4 of T2 data

has a negative effect on the quality of the analysis. In our data sets, it appears that at least 5 months, but preferably 6 months or longer, of data are needed for a reasonable result. Analyses of 1- to 4-month periods using Approach #1 are not robust.

Contrary to Approach #1, the binning-based comparison can be performed on far fewer data. Even 1 month's worth of data is sufficient. However, one needs to keep in mind that the binning-based comparison does not control well for the weather-causing discrepancy between the pair of data sets. When the weather conditions before and after a technical action are drastically different, the binning-based analysis is also not robust. So we generally recommend a 12-month comparison period, or something close, when applying the binning-based comparison.

Looking at Figure 6, one can observe that when the comparison period is long enough, the binning-based comparison and Approach #1 yield quite comparable results. As the comparison periods are shortened, the differences between the two methods become increasingly substantial. The difference is particularly difficult to reconcile for the first 4 months. The imperfection of both the binning-based comparison and Approach #1 contributes to the difference.

For Approach #1, as we said, the fewer data in the shorter period deteriorates the performance of the method. If we look at the 7-month or longer period, the analysis outcomes are reasonably stable (not sensitive to data length, which is desirable). The binning-based comparison is only relatively stable for 11- or 12-month and becomes sensitive when a shorter period is used. Its quantification value keeps increasing until it reaches the peak when using a 3- or 4-month period in comparison. We believe that this pattern is due to the imperfect control of the weather effect in the binning-based comparison. In other words, the increasing pattern of the green bars in Figure 6 is due to the weather effect.

To see this, consider the following. The time point separating Period 3 and Period 4 is in August–September of 2019; see Table 2. This means that the 4 months before are spring and summer, whereas the 4 months after are fall and winter. The fall–winter data have more favorable wind speed and cooler ambient temperature, whereas the spring–summer data are the opposite. We include in Figure 7, for the 4 months closest to the LEP repair time, the probability density functions of the wind speed and temperature, and the energy production before and after. It is apparent that not only did Period 4 (after) have stronger winds, it was also significantly colder. The wind turbines naturally produced more energy in Period 4 and the binning-based comparison is affected by this weather effect.

When the period of comparison is long enough, especially with all seasons included like when using the full-year data before and after, both Approach #1 and the binning-based comparison suggest that T2 indeed had a better performance in Period 4 than in Period 3. Recall that when using Approach #1, the weather effect is supposed to be controlled for already. What this means is that the difference with a 12-month comparison period, 5.02%, is attributed to wind turbine performance change. This value is large enough and cannot be dismissed as random fluctuation.

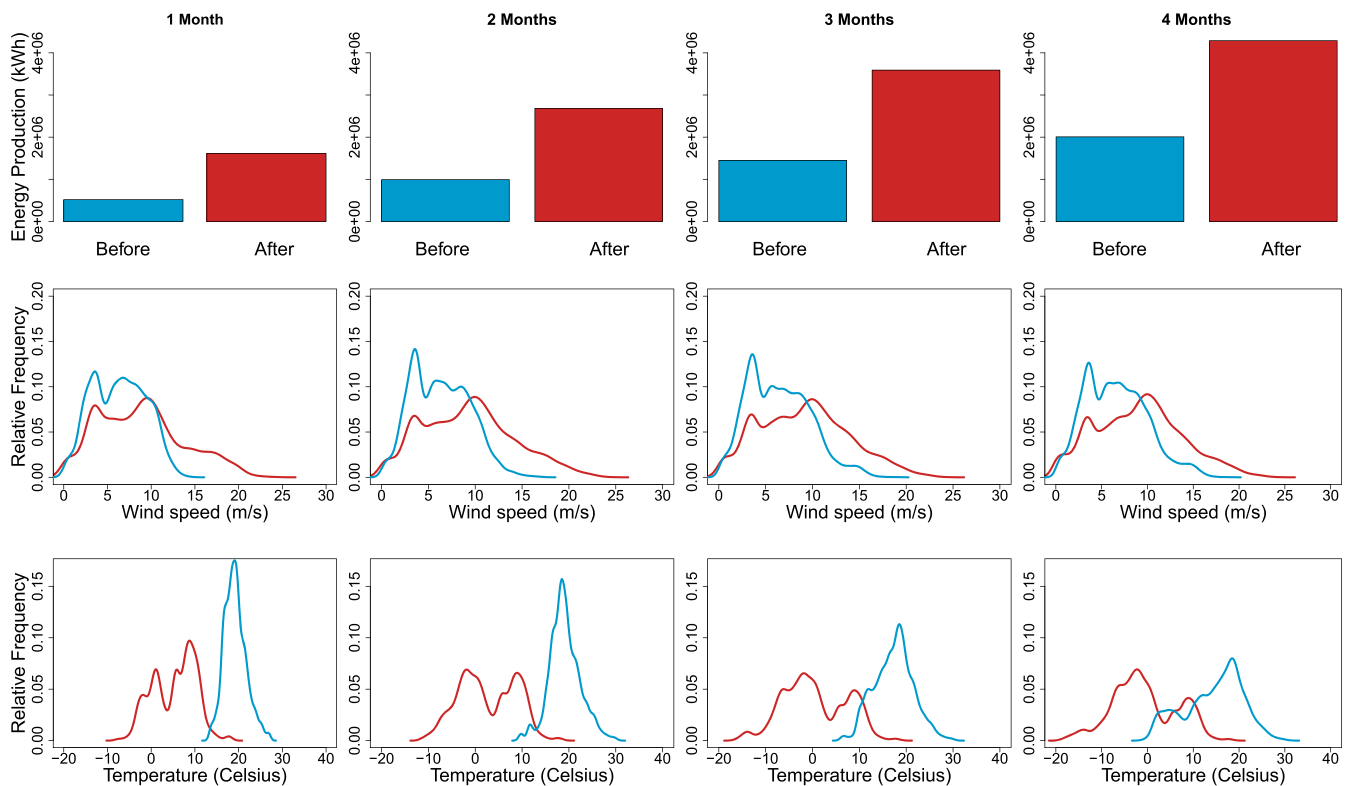


**FIGURE 7** Top row: total energy production by T2 for 1- to 4-month periods before and after LEP repair. Middle row: probability density functions of wind speed before and after LEP repair. Bottom row: probability density functions of ambient temperature before and after LEP repair. The blue color represents Period 3 (before), whereas the red color represents Period 4 (after)

Random fluctuation generally accounts for 1%–1.5%. Deducting 1.5% from 5.02%, one is still left with a positive 3.52%, a rather sizeable improvement. But recall that T2 did not undertake LEP repair. There were no other recorded actions on its blade in Period 3, in Period 4, or in between. Our team conducted a follow-up study, looking into what happened to T2.

Nevertheless, we want to make sure that the results so far obtained are not artifacts. The next several subsections present detailed analysis and validation to lend credibility to our analysis approach and outcome.

### 4.3 | Turbine performance change before and after LEP repair

In order to double check the results obtained from using Approach #1, we use the delta energy decomposition method (Approach #2) to re-estimate the performance change before and after the time point of LEP repair. With this approach, we expect to understand not only a wind turbine's intrinsic performance, but also how the weather affects individual turbines. Recall that to perform the delta energy decomposition, there are a few preprocessing steps to take; see Section 3.3. After the preprocessing, all turbines have the same data size (50,863 data points for each period), corresponding to 12 months. In this part of the study, we focus on T1–T4 while excluding T5.

We obtain  $\Delta\hat{E}_{weather}$  and  $\Delta\hat{E}_{turbine}$  by applying Equations (9) and 11, respectively. The estimate of  $\Delta\hat{E}$  is obtained directly using Equation (5). We also apply Approach #1 to the preprocessed data. It yields its own version of delta power for turbines, just as the method did in the previous sections. Because we use a constant 10-min time stamped data points in our delta energy analysis, the percentage delta power and percentage delta energy are comparable. The new delta power values differ slightly from those presented in Table 4, as the results in Table 4 are obtained from the data without the type of data preprocessing specified in Section 3.3.

Table 5 presents the results of delta energy decomposition from Approach #2 and the updated delta power result using Approach #1 on the preprocessed data.

We would like to note a few things. First, the last row of Table 5, that is, the updated Approach #1 result, indeed differs from the Approach #1 values in Table 4, which are 1.19%, 5.02%, –0.89%, and 3.18%, respectively, for T1–T4. Second,  $\Delta\hat{E}_{weather}$  and  $\Delta\hat{E}_{turbine}$  based on Approach #2 do add to the amount of  $\Delta\hat{E}$ , as our decomposition formulation in Equations (9) and 11 guarantees. Third, the performance change of each turbine quantified by Approach #2 (the second last row) is close to the quantification produced by Approach #1 (the last row). These two sets of values are not expected to be the same, as the two quantification approaches went through very different formulations and calculations, yet they produce such consistent results. We believe the consistency in the analysis outcomes between the two approaches provides a strong cross-validation, boosting the robustness of the overall analysis.

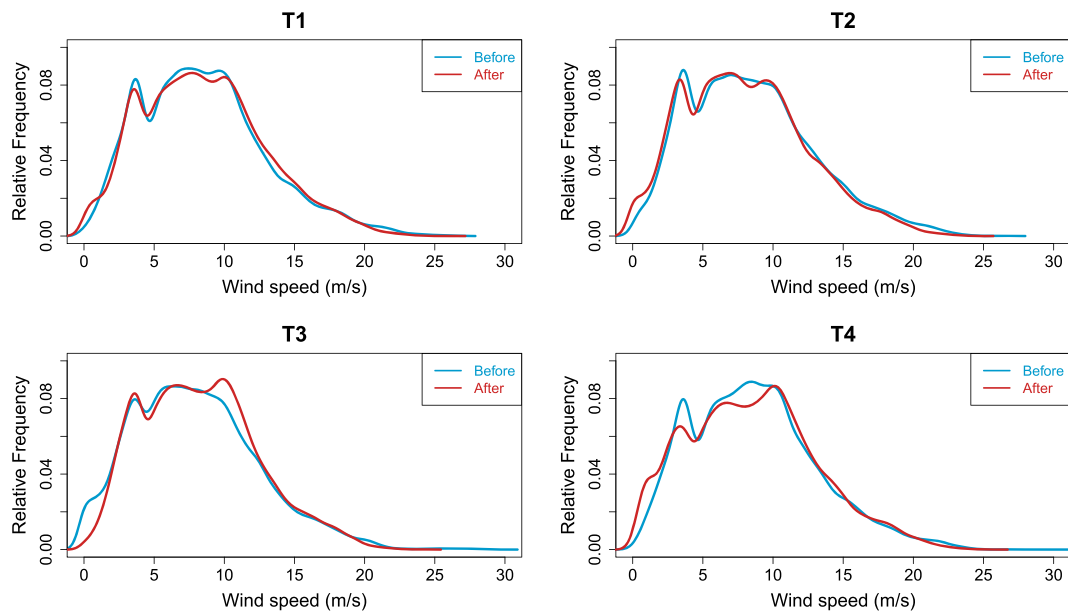
The benefit of Approach #2 is in its ability to separate the two effects in the overall delta energy calculation. Had someone used the direct delta energy for comparison (either  $\Delta E_{obs}$  or  $\Delta\hat{E}$ ), the outcomes would have been very different from those obtained from Approach #1. Take T2 as an example. The direct delta energy difference between Period 4 and Period 3 is 1.17%, whereas Approach #1 says the difference is 5.55%. A closer look shows that the 1.17% difference is the combined effect of the weather difference and the wind turbine's intrinsic change. The weather condition in Period 3 turned out to be more favorable for energy production. Should the ideal, no-change turbine operate in the two periods, the energy production would have reduced by 4.07%. But in reality, the energy production increased by 1.17%, implying that the turbine itself saw a positive 5.24% change. This 5.24% is Approach #2's quantification of T2's intrinsic performance change, close enough to and consistent with the 5.55% performance change quantified by Approach #1.

Table 5 also shows that the  $\Delta\hat{E}_{weather}$  effect is different on different turbines, although the four turbines are selected from the same neighborhood; see Figure 1. This may appear counterintuitive at first glance, but a closer examination indicates that the phenomenon is not unexpected. There are two main reasons behind this. The first reason is that while the weather conditions are indeed similar to these turbines, they are not the same. The second reason is that each turbine can react to the weather conditions in its own way, amplifying the already different weather conditions on energy production.

**TABLE 5** Weather and turbine effects decomposition using Approach #2

	T1	T2	T3	T4
$\Delta E_{obs}$	3.08%	1.17%	5.85%	2.85%
$\Delta\hat{E}$	3.08%	1.17%	5.85%	2.85%
$\Delta\hat{E}_{weather}$	1.30%	–4.07%	6.37%	–0.55%
$\Delta\hat{E}_{turbine}$	1.78%	5.24%	–0.52%	3.40%
Approach #1's power difference	1.50%	5.55%	–0.44%	3.63%

Note: A positive value means that the after period is better.



**FIGURE 8** Probability density functions of wind speed in the before and after periods for each wind turbine. In all plots, the blue lines represent the “before” period and the red lines represent the “after” period

To see the difference of the weather conditions, we plot in Figure 8 the pdfs of the wind speed measured on the four turbines. We would like to note again that the data sets from all turbines were already filtered to have the same time stamps and cover the full-year period before and after the LEP repair, so any difference that exists is not due to different inclusions of seasons.

One can observe that for T1 (top left), the Period 4 pdf, shown as the red line, is slightly to the right of Period 3, shown as the blue line, indicating that wind speed is more favorable in the “after” period. This is similar to what has been experienced by T3 (bottom left), but even more obviously for T3, especially around the rated wind speed. On the other hand, for T2 (top right), the Period 4 pdf is slightly to the left of the Period 3 pdf, indicating a less favorable wind speed in the “after” period. Not surprisingly,  $\Delta \hat{E}_{weather}$  for T1 and T3 is positive and that for T2 is negative. For T4 (bottom right), the difference between the two pdfs is most noticeable in the low-wind region close to or less than the cut-in wind speed. The quantification result shows that  $\Delta \hat{E}_{weather}$  for T4 is close to zero.

Through this follow-up analysis, particularly the employment of Approach #2 to cross validate the performance changes of the turbines, we are more confident that the previously obtained results are trustworthy, not artifacts introduced by model bias etc. But the change in T2 was certainly not due to LEP repairing, as T2 did not undertake the LEP repair action.

In order to understand the reason behind T2's improvement, we continued the work and investigated the drivetrain data. We noticed a drop in the drive-end bearing temperature around mid-November 2019, the time when the production performance started to change. Retrospective inspection showed that this change was due to a fix of potential leaks in gearbox lubricating oil (and topping up the oil). The lower temperature suggests a more efficient running of the gearbox, as lower temperature means smaller friction experienced by the bearing and less energy loss. In other words, our investigation shows that the positive change of T2 before and after the time point of LEP repair is genuine, not an artifact. It is due to the drivetrain effect, rather than the blades (as there was no blade action). We believe this study identified one of the cases in which an efficient running of the gearbox system benefits substantially the energy production performance. This finding is not entirely surprising, as such causal relationship has been suspected for a long time.

#### 4.4 | Power decomposition using Approach #1

This subsection explains how Approach #1 can be used to do a power decomposition analysis, similar to the energy decomposition done by Approach #2 in Table 5. This power decomposition is not presented in the original publication of Approach #1 but in a new contribution made by our team, inspired by our work on energy decomposition.

In order to use Approach #1 to decompose the power output to weather effect and turbine effect, we need to make use of two power outputs from the `ComparePCurve` function in the `DSWE` package: `mu1` and `mu2`. To understand what `mu1` and `mu2` mean, we need to explain the two-dimensional binning conducted to partition wind speed and ambient temperature.

Using the two input variables, we partition the two-dimensional region into 2500 small bins, 50 bins per input variable. The ranges of wind speed and temperature are decided by the input data,  $D^{(1)}$  and  $D^{(2)}$ ; for instance, the wind speed range can be from cut-in to cut-out wind speed and the temperature may be from  $-10^{\circ}\text{C}$  to  $40^{\circ}\text{C}$ . The 2500 bins partition the area into a very fine grid, and over each of the bins, we assume that the power output is a constant. The power for a specific bin can be calculated using the estimated power functions (either using  $\hat{f}^{(1)}(\cdot)$  or using  $\hat{f}^{(2)}(\cdot)$ ). The results are two vectors of power values, stored in  $\mu_1$  and  $\mu_2$  produced by the `ComparePCurve` function.

When one gathers the actual weather data from  $D^{(1)}$  and  $D^{(2)}$  and scatters them into the 2500 bins, the weather data are not evenly distributed. The relative proportion of the weather data in bin  $j$  is denoted by  $p_j$ , with all values of  $p_j$ 's adding to one over the entire 2500 bins. Figure 9 illustrates the two-dimensional binning and the meaning of  $\mu_1$ ,  $\mu_2$ , and  $p_j$ . Figure 9 uses only 36 bins, rather than 2500 bins, for the sake of illustration. The choice of 2500 is meant to create bins that are fine enough (i.e., a neighborhood small enough), so that the power in that bin can be reasonably assumed to be constant. When necessary, the number of bins can be easily adjusted, and the value of 2500 is just the default setting.

Still using Equations (5)–(13), but removing the time variable  $t$ , and replacing  $\hat{f}$  and  $x$  with  $\mu$  and  $p$ , respectively, we can calculate  $\Delta\hat{P}$ ,  $\Delta\hat{P}_{weather}$ , and  $\Delta\hat{P}_{turbine}$ , the counterparts of  $\Delta\hat{E}$ ,  $\Delta\hat{E}_{weather}$ , and  $\Delta\hat{E}_{turbine}$ , respectively, as follows:

$$\Delta\hat{P} = \sum_{j=1}^n \mu_j^{(2)} p_j^{(2)} - \sum_{j=1}^n \mu_j^{(1)} p_j^{(1)}, \tag{15}$$

$$\Delta\hat{P}_{weather} = \frac{1}{2} \left( \sum_{j=1}^n \mu_j^{(1)} p_j^{(2)} - \sum_{j=1}^n \mu_j^{(1)} p_j^{(1)} \right) + \frac{1}{2} \left( \sum_{j=1}^n \mu_j^{(2)} p_j^{(2)} - \sum_{j=1}^n \mu_j^{(2)} p_j^{(1)} \right), \tag{16}$$

$$\Delta\hat{P}_{turbine} = \frac{1}{2} \left( \sum_{j=1}^n \mu_j^{(2)} p_j^{(1)} - \sum_{j=1}^n \mu_j^{(1)} p_j^{(1)} \right) + \frac{1}{2} \left( \sum_{j=1}^n \mu_j^{(2)} p_j^{(2)} - \sum_{j=1}^n \mu_j^{(1)} p_j^{(2)} \right), \tag{17}$$

where  $\mu^{(1)}$  and  $\mu^{(2)}$  are the power outputs from the `DSWE` package that were originally labeled  $\mu_1$  and  $\mu_2$ , respectively,  $p_j^{(1)}$  and  $p_j^{(2)}$  are the density of the preprocessed data in the  $j^{\text{th}}$  bin,  $j$  and  $n$  are the index of and the total number of the bins. The  $\Delta\hat{P}$ ,  $\Delta\hat{P}_{weather}$ , and  $\Delta\hat{P}_{turbine}$  will be proportional to  $\Delta\hat{E}$ ,  $\Delta\hat{E}_{weather}$ , and  $\Delta\hat{E}_{turbine}$ , respectively, because the time,  $t_i$ , used previously to calculate energy is a constant of 10 min. When we

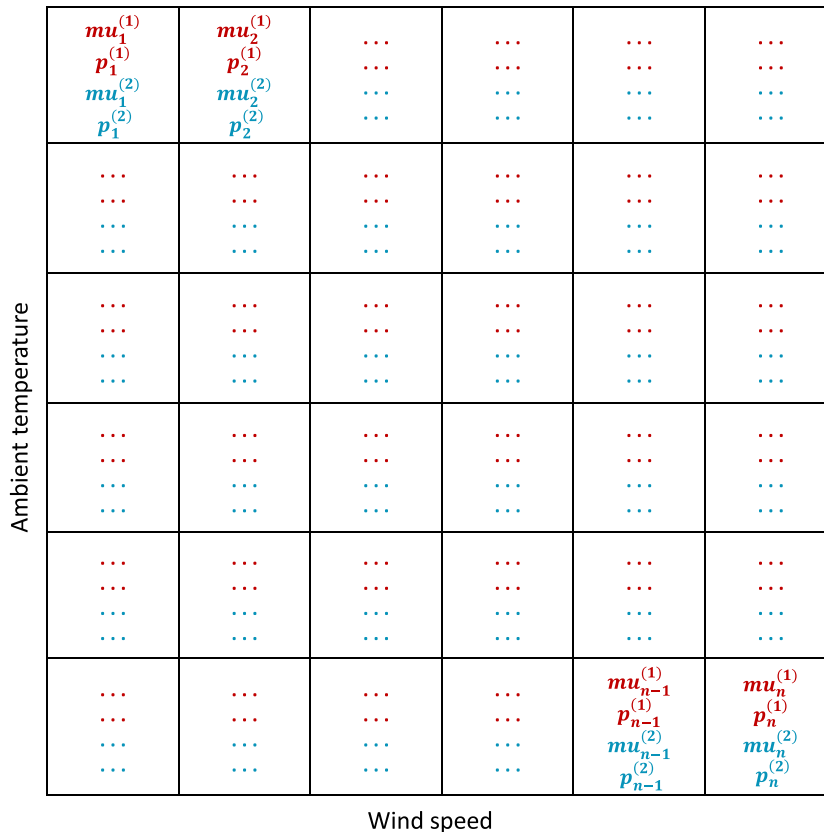


FIGURE 9 Illustration of two-dimensional binning and the meaning of  $\mu_1$ ,  $\mu_2$ , and  $p_j$

compute the percentage expression as in Equations (12) and 13, the time,  $t_i$ , is cancelled out from the denominator and the numerator. In this sense, the power-based percentage and energy-based percentage are comparable. In the latter tables, the notations,  $\Delta\hat{E}$ ,  $\Delta\hat{E}_{weather}$ , and  $\Delta\hat{E}_{turbine}$ , are used for the sake of simplicity.

Let us use Approach #1 to obtain the decomposition for each wind turbine, still comparing Period 3 and Period 4. The results are presented in Table 6, in which the first row,  $\Delta E_{obs}$ , is taken directly from the previous delta energy analysis. Comparing the results in this table with those in Table 5, one can see that the results still show a good degree of agreement.

#### 4.5 | Turbine pairwise performance comparison

Previously, we conducted a pairwise comparison involving a turbine but two periods; that can be referred to as *period pairwise comparison*. We can certainly conduct a pairwise comparison involving two turbines over the same period, which would be referred to as *turbine pairwise comparison*. Combining the period pairwise comparison and turbine pairwise comparison produces a comparison involving two turbines over two periods. Both Approach #1 and Approach #2 can be used to conduct these analyses. The analysis results show again a high degree of agreement between these two approaches, which is reassuring. For notational simplicity, we write Period 1 as P1, Period 2 as P2, and so forth.

The turbine pairwise comparison can be directly obtained from Table 5 and Table 6. For example, using the results from Approach #1 in Table 6 and taking the difference between the turbine effect values under T1 and T4, one gets 1.84% (=3.31% – 1.47%). What the 1.84% means is that going from P3 to P4, T4 sees a greater improvement than T1. The extra improvement experienced by T4, relative to that experienced by T1, is 1.84%. The same analysis can be conducted by using Approach #2, and a similar result is expected.

Please note that the above analysis goes through the route of a period pairwise comparison first and then a turbine pairwise comparison later. We label this as the P2T route. Understandably, we can do an analysis between two turbines under the same period and then compare the turbine difference across two periods, namely, a turbine pairwise comparison first and then a period pairwise comparison later. We label the latter approach as the T2P route.

It is easier to explain how the T2P approach works using Table 7. Take the first row for example. The first row is about the turbine pair of T1 and T2. When P3 is concerned,  $D^{(1)}$  is the T1 data in P3 and  $D^{(2)}$  is the T2 data in P3. Feeding  $D^{(1)}$  and  $D^{(2)}$  into the same `ComparePCurve` function in the `DSWE` package will produce the estimate of the two turbines' difference for P3, which is –0.27% in Table 7, with T2 slightly worse. Moving to P4, the same analysis can be done, producing the T2–T1 difference for P4, which is 3.16%. Then, taking the difference between these two values produces the estimate of the difference between T2 and T1, as both turbines go from P3 to P4. The next three columns of the same row are the same analysis but based on Approach #2.

Recall that we have used the P2T approach above to estimate the same thing; those estimates are included in the last two columns of Table 7. For example, using Approach #1, the P2T estimate of T4–T1 difference when going from P3 to P4 is 1.84%; this is the value showing up in the second to last column and corresponding to the row of (T1, T4).

**TABLE 6** Individual wind turbine effect decomposition based on Approach #1

Delta energy	T1	T2	T3	T4
$\Delta E_{obs}$	3.08%	1.17%	5.85%	2.85%
$\Delta\hat{E}$	2.58%	1.01%	6.05%	2.56%
$\Delta\hat{E}_{weather}$	1.11%	–4.25%	6.49%	–0.75%
$\Delta\hat{E}_{turbine}$	1.47%	5.26%	–0.44%	3.31%

**TABLE 7** Turbine effects ( $\Delta\hat{E}_{turbine}$ ) in the pairwise comparisons

Turbine pair	T2P based on Approach #1			T2P based on Approach #2			P2T estimate of P4–P3	
	P3	P4	P4–P3	P3	P4	P4–P3	Approach #1	Approach #2
(T1,T2)	–0.27%	3.16%	3.43%	–0.39%	3.04%	3.43%	3.79%	3.45%
(T1,T3)	2.23%	0.66%	–1.57%	2.34%	–0.10%	–2.44%	–1.90%	–2.30%
(T1,T4)	–3.32%	–1.25%	2.07%	–3.25%	–1.41%	1.84%	1.84%	1.61%
(T2,T3)	2.77%	–2.86%	–5.63%	2.69%	–3.13%	–5.82%	–5.70%	–5.76%
(T2,T4)	–2.77%	–4.17%	–1.40%	–2.81%	–4.27%	–1.46%	–1.95%	–1.84%
(T3,T4)	–5.52%	–1.58%	3.95%	–5.59%	–1.29%	4.30%	3.75%	3.92%

The same analysis is conducted to quantify the weather effects, the results of which are in Table 8.

We mean to compare the fourth, seventh, eighth, and ninth columns in Tables 8 and 7. These estimates appear to be highly consistent, which is the reassuring aspect we emphasized above.

By setting T1 performance in P3 as the baseline, we can summarize the performance of turbines relative to each other in both P3 and P4. Considering that the two approaches yield highly comparable outcomes, it is fine to use either approach to get the turbine performance estimate. We choose to use Approach #1. The result is presented in Figure 10. To understand the plot, consider T2. Its performance in Period 3 is 0.27% worse than T1 (the first row of Table 7, under Approach #1, then P3). Its own performance change from Period 3 to Period 4 is 5.26%, according to Table 6 (last row, under T2). T1 itself sees a positive improvement of 1.47% from Period 3 to Period 4, according to Table 6 (last row, under T1). This suggests that in Period 4, the difference between T2 and T1 becomes 3.52% ( $= -0.27\% + 5.26\% - 1.47\%$ ), with T2 better than T1. The corresponding value in Table 7 is 3.43% (T2P) or 3.79% (P2T); all these estimates are close to each other.

Based on Figure 10, three turbines experienced positive changes and only T3 declined in the last period. Compared to all, T4 has always had the lowest performance in both periods, even with its noticeable improvement in the last period. Despite the disadvantageous weather experienced by T2, it still showed a performance improvement in the last period. In fact, it outperformed the other three turbines in the end.

#### 4.6 | Quantification of energy production change at below-rated wind speed

The LEP application or damages on the blades are expected to affect the aerodynamics of the blades. To quantify such effects on the energy production, one needs to focus on the below-rated region of the power curve, which is below 1800 kW on these turbines. For this reason, we perform additional comparisons using Approach #1 to the data points selected for the power output between 25 and 1800 kW. We expect to see a greater difference in this comparison, when contrasted with the comparisons over the entire region.

**TABLE 8** Weather effects ( $\Delta\hat{E}_{weather}$ ) in the pairwise comparisons

Turbine pair	T2P based on Approach #1			T2P based on Approach #2			P2T estimate of P4–P3	
	P3	P4	P4–P3	P3	P4	P4–P3	Approach #1	Approach #2
(T1,T2)	−1.97%	−7.23%	−5.26%	−1.77%	−7.11%	−5.34%	−5.36%	−5.37%
(T1,T3)	−8.92%	−3.52%	5.40%	−8.55%	−3.35%	5.20%	5.38%	5.07%
(T1,T4)	3.00%	1.04%	−1.96%	3.15%	1.07%	−2.08%	−1.86%	−1.85%
(T2,T3)	−6.93%	3.79%	10.72%	−6.75%	3.75%	10.50%	10.74%	10.43%
(T2,T4)	4.94%	8.12%	3.18%	4.87%	8.00%	3.13%	3.50%	3.52%
(T3,T4)	11.95%	4.59%	−7.36%	11.70%	4.40%	−7.30%	−7.24%	−6.92%

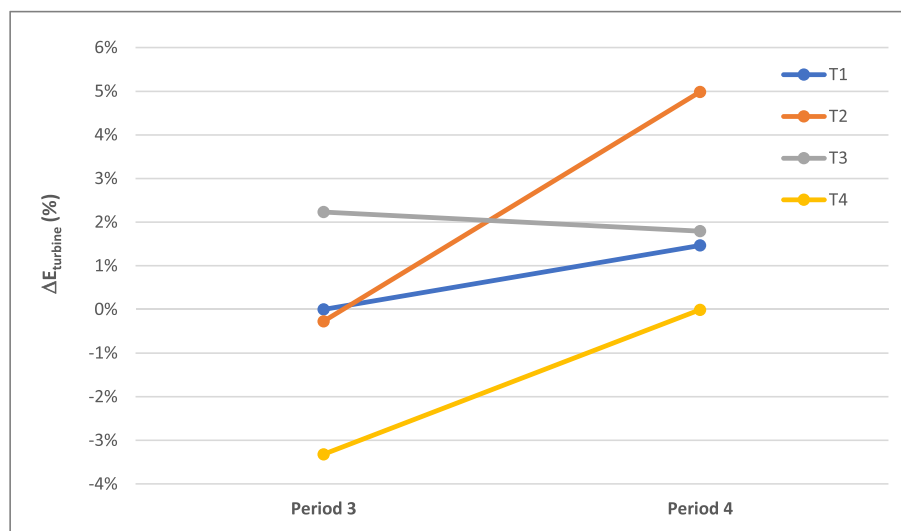


**FIGURE 10** The performance of four turbines (T1 to T4) in Period 3 and Period 4. T1 in Period 3 is used as the baseline for all



**TABLE 9** Turbine performance difference between Period 3 and Period 4 over different regions

Compared region	Weighted power difference				Weighted statistical power difference			
	T1	T2	T3	T4	T1	T2	T3	T4
Entire region	1.50%	5.55%	-0.44%	3.63%	0.69%	4.21%	-0.16%	2.01%
Low-power region	3.29%	14.16%	-2.48%	7.32%	0.83%	12.02%	-1.29%	5.77%

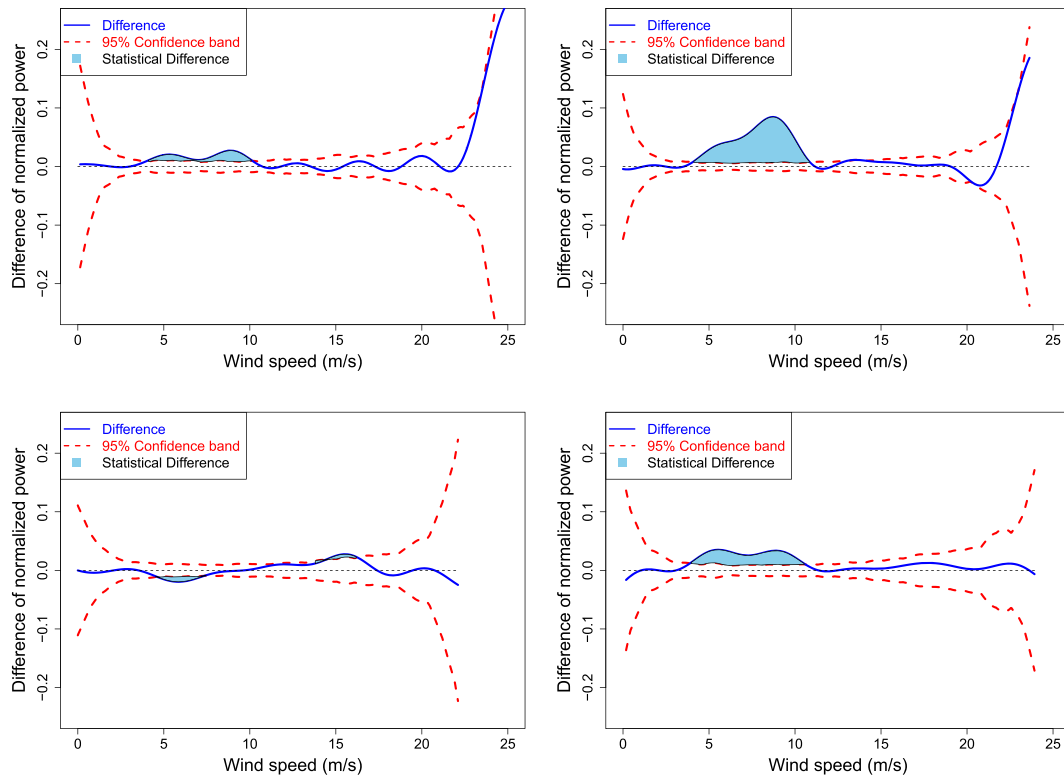


**FIGURE 11** Significant difference in power production over wind speed regions. Top Left: T1; Bottom Left: T3; Top Right: T2; Bottom Right: T4

Using again the LEP repair as a reference point, Table 9 presents the power difference between Period 3 and Period 4 for four turbines (T1 to T4) in both the entire region and low-power region (i.e., between 25 and 1800 kW). The result confirms that the most difference in the power production in fact happened in the low-power region.

The R package, *DSWE*, has an embedded function that can help visualize the difference in a comparison over the wind speed region. The result in terms of weighted statistical difference is presented in Figure 11, where the blue line is the power production difference between two periods for a turbine and the red dashed lines are the 95% confidence intervals of the difference. When any portion of the blue line is outside the red dashed lines (either above or below), it means that portion is statistically significant. The light blue shaded area corresponds to the statistical difference; see the discussion surrounding Figure 4.

We found that for T1, T2, and T4, the difference occurred mostly or entirely in the wind speed region of 5–10 m/s. In T2, a small part of the difference also occurred in the region near the cut-out wind speed. These turbines also have a clear positive performance change. For T3, the difference happened at two different wind speed regions: one positive and one negative. The combined effect is nearly zero after removing the noise fluctuation.

## 5 | CONCLUSION

We apply two different methods for turbine performance analysis to understand the effects of LEP application—one from the existing method and our own proposed decomposition method. The data sets used are of five turbines on a small inland wind farm, and each includes more than

five year's worth of data. During this period, three blade-related technical actions were performed: an action of LEP was applied to all five turbines in 2016, one of the turbines had its blades repainted in 2017, and four of the turbines had LEP repairs in 2019.

In terms of the methods applied, the decomposition approach demonstrates its merit. Using the total energy in a direct comparison carries more of the weather effects than the turbine effects, and thus exhibits a strong pattern of seasonality. Our decomposition approach is able to remove the weather effects and reveal the turbine's own performance changes. We compare the proposed energy decomposition approach with the existing performance quantification procedure<sup>7</sup> and found that the two methods produce consistent outcomes, thereby cross-validating each other.

Through our analysis, we found that only one turbine benefited positively from the first LEP application, whereas the other four turbines suffered a small loss (0.82% in average) in performance. In the third technical change, we detected positive improvements in more than one turbine, but these improvements may not be due to LEP repairing because the turbine (T2) that experienced the greatest improvement turns out to be the one on which the LEP repair was not undertaken. Further analysis of T2 data indicates that its improvement is more likely attributed to the changes in drivetrain.

## ACKNOWLEDGEMENTS

Latiffianti's research is supported by a Fulbright Scholarship in collaboration with the Indonesian Government. Ding's research is partially supported by NSF grants IIS-1741173 I and CCF-1934904. This work was authored (in part) by the National Renewable Energy Laboratory, operated by Alliance for Sustainable Energy, LLC, under Contract No. DE-AC36-08GO28308 for the U.S. Department of Energy. Funding provided by the U.S. Department of Energy Office of Energy Efficiency and Renewable Energy Wind Energy Technologies Office. The views expressed in the article do not necessarily represent the views of the DOE or the U.S. Government. The U.S. Government retains and the publisher, by accepting the article for publication, acknowledges that the U.S. Government retains a nonexclusive, paid-up, irrevocable, worldwide license to publish or reproduce the published form of this work, or allow others to do so, for U.S. Government purposes.

## ORCID

Effi Latiffianti  <https://orcid.org/0000-0003-1523-6035>

Yu Ding  <https://orcid.org/0000-0001-6936-074X>

## REFERENCES

1. US Energy Information Administration (EIA). Electricity explained—Electricity in the United States, US Energy Information Administration (EIA); 2021. [10.1002/energyexplained/electricity/electricity-in-the-us.php](https://www.eia.gov/energyexplained/electricity/electricity-in-the-us.php)
2. Staffell I, Green R. How does wind farm performance decline with age? *Renew Energy*. 2014;66:775-786.
3. Herring R, Dyer K, Martin F, Ward C. The increasing importance of leading edge erosion and a review of existing protection solutions. *Renew Sustain Energy Rev*. 2019;115:109382.1-109382.13.
4. Ding Y. *Data Science for Wind Energy*. Boca Raton, FL, USA: Chapman & Hall; 2019.
5. Lee G, Ding Y, Xie L, Genton MG. A kernel plus method for quantifying wind turbine performance upgrades. *Wind Energy*. 2015;18(7):1207-1219. [10.1002/we.1755](https://doi.org/10.1002/we.1755)
6. Shin YE, Ding Y, Huang JZ. Covariate matching methods for testing and quantifying wind turbine upgrades. *The Ann Appl Stat*. 2018;12(2):1271-1292. [10.1214/17-AOAS1109](https://doi.org/10.1214/17-AOAS1109)
7. Ding Y, Kumar N, Prakash A, Kio AE, Liu X, Liu L, Li Q. A case study of space-time performance comparison of wind turbines on a wind farm. *Renew Energy*. 2021;171:735-746. [10.1016/j.renene.2021.02.136](https://doi.org/10.1016/j.renene.2021.02.136)
8. MacPhee DW, Beyene A. Performance analysis of a small wind turbine equipped with flexible blades. *Renew Energy*. 2019;132:497-508.
9. Charabi Y, Abdul-Wahab S. Wind turbine performance analysis for energy cost minimization. *Renew: Wind, Water, Solar*. 2020;7(5):1-11. [10.1186/s40807-020-00062-7.pdf](https://doi.org/10.1186/s40807-020-00062-7.pdf)
10. Google. Wind energy institute of canada. [Online].
11. Pearl J. Causal inference in statistics: an overview. *Stat Surv*. 2009;3:96-146. [10.1214/09-SS057](https://doi.org/10.1214/09-SS057)
12. Prakash A, Tuo R & Ding Y Gaussian process-aided function comparison using noisy scattered data. 2022;64:92-102. [10.1080/00401706.2021.1905073](https://doi.org/10.1080/00401706.2021.1905073)
13. Kumar N, Prakash A, Ding Y. DSWE: Data Science for Wind Energy, R Package Github Repository, Version 1.3.4. 2020. [10.1002/TAMU-AML/DSWE-Package](https://doi.org/10.1002/TAMU-AML/DSWE-Package)
14. Jin JY, Karlsson T & Virk MS Wind turbine ice detection using AEP loss method—a case study. *Wind Energy*. 2021. [10.5194/wes-2021-55](https://doi.org/10.5194/wes-2021-55)
15. Ouyang T, Kusiak A, He Y. Modeling wind-turbine power curve: a data partitioning and mining approach. *Renew Energy*. 2017;102:1-8.
16. Pei S, Li Y. Wind turbine power curve modeling with a hybrid machine learning technique. *Appl Sci*. 2019;9(22):4930.1-4930.18.
17. Janssens O, Noppe N, Devriendt C, de Walle RV, Hoecke SV. Data-driven multivariate power curve modeling of offshore wind turbines. *Eng Appl Artif Intell*. 2016;55:331-338.
18. Prakash A, Tuo R, Ding Y. The temporal overfitting problem with applications in wind power curve modeling. arXiv preprint. 2021. [10.1002/abs/2012.01349](https://doi.org/10.1002/abs/2012.01349)
19. Pandit R, Infield D. Gaussian process operational curves for wind turbine condition monitoring. *Energies*. 2018;11(7):1631.1-1631.20.
20. Rogers TJ, Gardner P, Dervilis N, Worden K, Maguire AE, Papatheou E, Cross EJ. Probabilistic modelling of wind turbine power curves with application of heteroscedastic gaussian process regression. *Renew Energy*. 2020;148:1124-1136.

21. Mehrjoo M, Jafari Jozani M, Pawlak M. Wind turbine power curve modeling for reliable power prediction using monotonic regression. *Renew Energy*. 2020;147:214-222.
22. Goudarzi A, Davidson IE, Ahmadi A, Venayagamoorthy GK. Intelligent analysis of wind turbine power curve models. In: 2014 IEEE Symposium on Computational Intelligence Applications in Smart Grid (CIASG); 2014:1-7.
23. Sareen A, Sapre CA, Selig MS. Effects of leading edge protection tape on wind turbine blade performance. *Wind Eng*. 2012;36(5):525-534.
24. International Electrotechnical Commission (IEC). *IEC 61400-12-1 ed 1, wind turbines-part 12-1: Power performance measurements of electricity producing wind turbines*. Geneva, Switzerland: IEC; 2005.
25. Lee G, Ding Y, Genton MG, Xie L. Power curve estimation with multivariate environmental factors for inland and offshore wind farms. *J Am Stat Assoc*. 2015;110(509):56-67. <https://doi.org/10.1080/01621459.2014.977385>

**How to cite this article:** Latiffianti E, Ding Y, Sheng S, Williams L, Morshedizadeh M, Rodgers M. Analysis of leading edge protection application on wind turbine performance through energy and power decomposition approaches. *Wind Energy*. 2022;25(7):1203-1221. doi:[10.1002/we.2722](https://doi.org/10.1002/we.2722)